

Defining super-enhancers by highly ranked histone H4 multi-acetylation levels identifies transcription factors associated with glioblastoma stem-like properties

Nando D. Das¹, Jen-Chien Chang², Chung-Chau Hon³, S. Thomas Kelly², Shinsuke Ito⁴, Marina Lizio³, Bogumil Kaczkowski⁵, Hisami Watanabe¹, Keisuke Katsushima⁶, Atsushi Natsume⁷, Haruhiko Koseki^{4,8}, Yutaka Kondo⁶, Aki Minoda^{2,9} and Takashi Umehara^{1,10,*}

¹Laboratory for Epigenetics Drug Discovery, RIKEN Center for Biosystems Dynamics Research, Yokohama, Japan; ²Laboratory for Cellular Epigenomics, RIKEN Center for Integrative Medical Sciences (IMS), Yokohama, Japan; ³Laboratory for Genome Information Analysis, RIKEN IMS, Yokohama, Japan; ⁴Laboratory of Developmental Genetics, RIKEN IMS, Yokohama, Japan; ⁵Laboratory for Applied Regulatory Genomics Network Analysis, RIKEN IMS, Yokohama, Japan; ⁶Division of Cancer Biology, Nagoya University Graduate School of Medicine, Nagoya, Japan; ⁷Department of Neurosurgery, Nagoya University Graduate School of Medicine, Nagoya, Japan; ⁸Immune Regulation, Advanced Research Departments, Graduate School of Medicine, Chiba University, Chiba, Japan; ⁹Department of Cell Biology, Faculty of Science, Radboud Institute for Molecular Life Sciences, Radboud University, Nijmegen, Netherlands, ¹⁰PRESTO, Japan Science and Technology Agency, Kawaguchi, Saitama, Japan

*Correspondence and requests for materials should be addressed to T.U. (email: takashi.umehara@riken.jp).

Supplementary Figures

Figure S1. Identification of regions that bind H4K5acK8ac preferentially over H3K27ac.

Figure S2. Effect of JQ1 on genome-wide enrichment of BRD4, H3K27ac, and H4K5acK8ac across glial cell lines.

Figure S3. Effect of H4K5acK8ac level in regulatory elements on changes in gene expression upon JQ1 treatment in three glial cell lines.

Figure S4. Effect of JQ1 on specific genes and various biological pathways and molecular functions across the three glial cell lines.

Figure S5. Defining super-enhancers (SEs) by H4K5acK8ac enrichment ranking in 0316-GSC, U87, and C13NJ cells.

Figure S6. CRISPR-Cas9-mediated genome editing strategy of H4K5acK8ac-preferred super-enhancers (SEs) in 0316-GSC cells.

Figure S7. CRISPR-Cas9-mediated genome editing of *HOXA7* super-enhancers (SEs) in 0316-GSC cells.

Figure S8. CRISPR-Cas9-mediated genome editing of H3K27ac-preferred super-enhancers (SEs) in 0316-GSC cells.

Figure S9. Source data for cropped gel images.

Figure S1

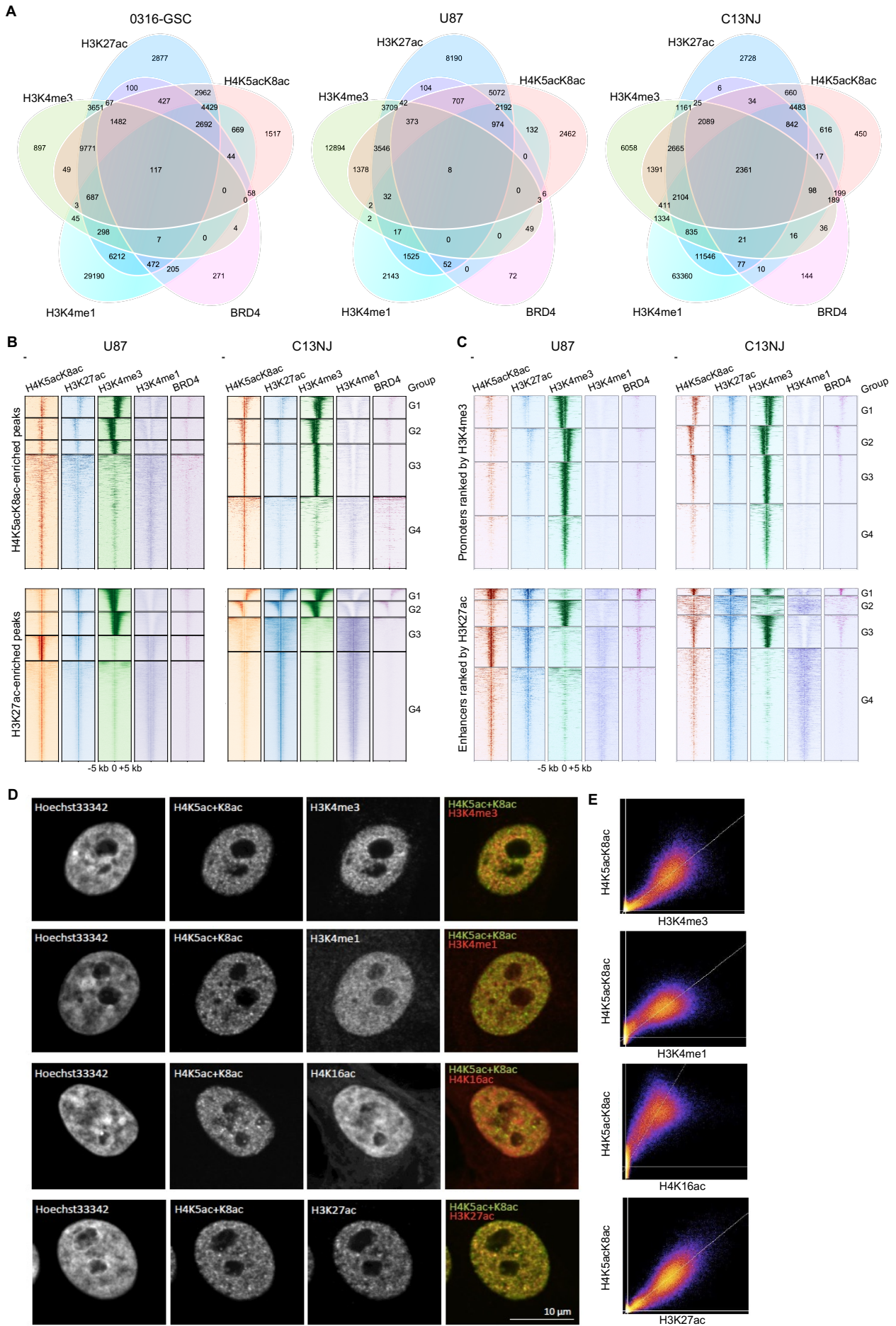


Figure S1 (continued)

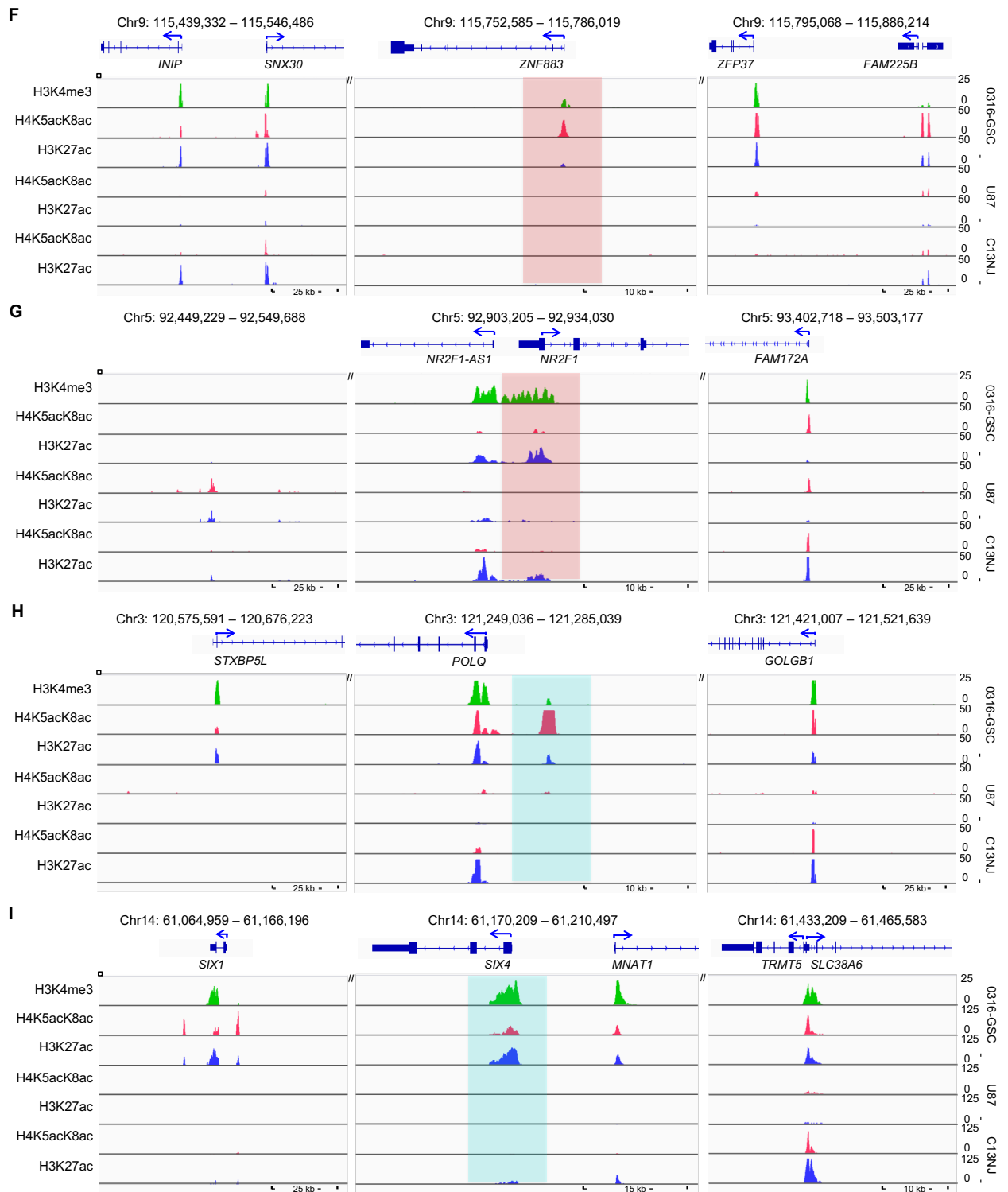


Figure S1. Identification of regions that bind H4K5acK8ac preferentially over H3K27ac. **A** Venn diagrams representing the overlap of ChIP-seq peaks of H4K5acK8ac with H3K27ac, H3K4me1, H3K4me3, and BRD4 across O316-GSC, U87, and C13NJ cell lines. **B** and **C** Heatmaps representing different ChIP-seq datasets (H4K5acK8ac, H3K27ac, H3K4me3, H3K4me1, and BRD4) in U87 and C13NJ cell lines. Data are from within \pm 5-kb from the summit of H4K5acK8ac-enriched peaks (upper, **B**) and H3K27ac-enriched peaks (lower, **B**), and promoters defined by H3K4me3 at the promoters (upper, **C**) and enhancers defined by H3K27ac located outside a promoter (lower, **C**). Each row represents a single peak. Color density indicates the average enrichment of each mark at the selected regions. H4K5acK8ac- or H3K27ac-enriched peaks (**B**) and promoters or enhancers (**C**) are each clustered into four groups (G1 to G4) according to the ChIP-seq profiles. **D** Immunostaining analysis demonstrating the colocalization of H4K5acK8ac with H3K4me3, H3K4me1, H4K16ac, and H3K27ac marks in U87 cells. Hoechst 33342 was used for nuclear staining. Scale bar, 10 μ m. **E** Correlation of immunofluorescence signal between H4K5acK8ac and other specific marks in U87 cells. **F–I** Representative O316-GSC-specific ChIP-seq tracks of H4K5acK8ac-preferred (\log_2 fold-change (FC) [H4K5acK8ac/H3K27ac] > 1) and H3K27ac-preferred (\log_2 FC [H4K5acK8ac/H3K27ac] < -1) promoters (**F** and **G**) and enhancers (**H** and **I**).

Figure S2

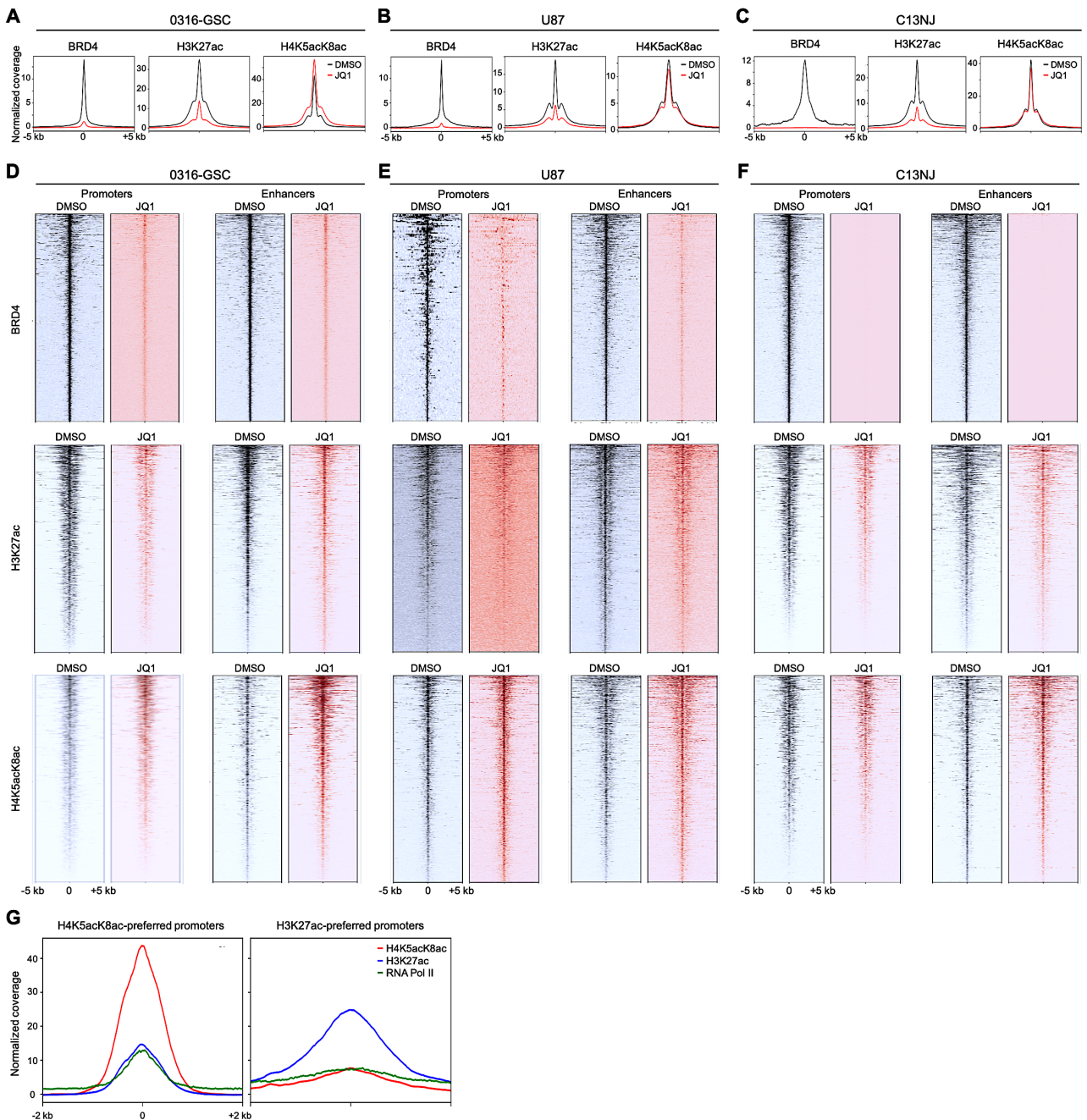


Figure S2. Effect of JQ1 on genome-wide enrichment of BRD4, H3K27ac, and H4K5acK8ac across glioblastoma cell lines. **A–C** ChIP-seq meta-profiles for dimethyl sulfoxide (DMSO; vehicle control) and JQ1-treated cells showing the average read counts (reads per million; RPM) of ± 5 kb regions from the summit of BRD4-, H3K27ac-, and H4K5acK8ac-enrichment. Compared with treatment with DMSO, treatment with 5 μ M JQ1 for 24 h led to a global loss of BRD4 and H3K27ac across the three cell lines, and the enrichment of H4K5acK8ac in 0316-GSC but not U87 or C13NJ cells. **D–F** Heatmaps of ChIP-seq datasets of BRD4, H3K27ac, and H4K5acK8ac upon JQ1 treatment in 0316-GSC cells (**D**), U87 (**E**), and C13NJ (**F**) cells within ± 5 kb from the summit of active promoters (defined by cell type-specific H3K4me3) (left) or active enhancers (defined by cell type-specific H3K27ac located outside promoter) (right). Each row represents a single peak. Color density indicates the average enrichment of each mark at promoters and enhancers. **G** Colocalization of RNAP II with promoters. ChIP-seq meta-profiles show the association of RNAP II (green) with H4K5acK8ac-preferred (red) and H3K27ac-preferred (blue) promoters.

Figure S3

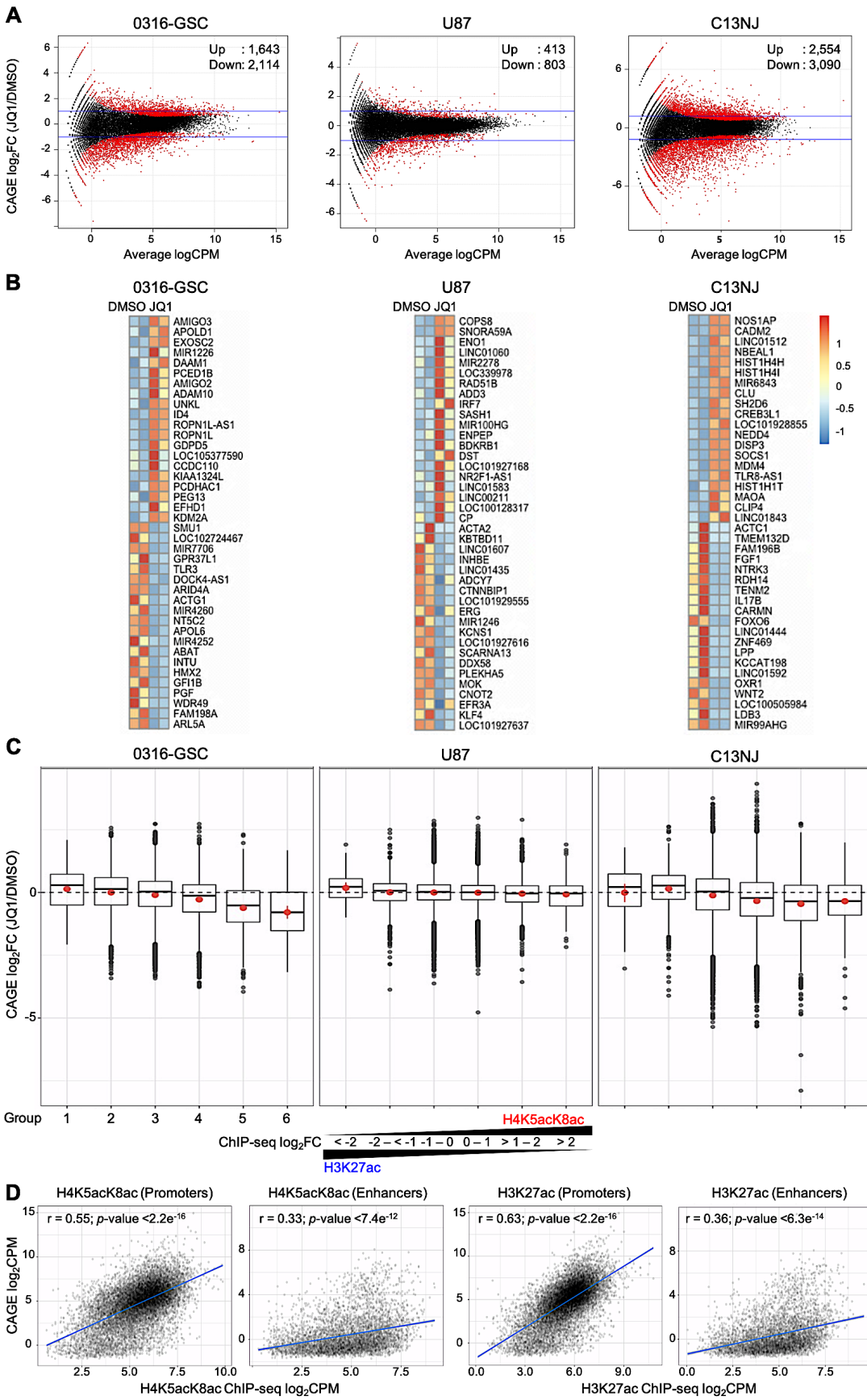


Figure S3. Effect of H4K5acK8ac level in regulatory elements on changes in gene expression upon JQ1 treatment in three glial cell lines. **A** Relative expression of genes upon JQ1 treatment. Numbers of genes significantly upregulated or downregulated by 24-h treatment with 5 μ M JQ1 relative to DMSO (false discovery rate < 0.05 ; CAGE \log_2 FC [JQ1/DMSO] > 0.5 or < -0.5 , respectively) are shown for each of the three cell lines. **B** Heatmaps of the top 20 genes differentially upregulated and top 20 genes differentially downregulated by JQ1 are shown based on the ranking of CAGE \log_2 FC in each cell line. **C** Box plots of relative expression of genes upon JQ1 treatment for promoters or enhancers grouped by their level of enrichment of H4K5acK8ac over H3K27ac. Groups 1–3 are defined by ChIP-seq \log_2 FC (H4K5acK8ac/H3K27ac) of < -2 , -2 to < -1 , and -1 to 0, respectively (H3K27ac-preferred; \log_2 FC < -1). Groups 4–6 are defined by ChIP-seq \log_2 FC 0 to 1, >1 to 2, and >2 , respectively (H4K5acK8ac-preferred; \log_2 FC > 1). **D** Scatter plots of the change in gene expression upon JQ1 treatment (CAGE \log_2 FC) versus levels of histone modifications (ChIP-seq \log_2 CPM) for genes associated with H4K5acK8ac-preferred and H3K27ac-preferred promoters or enhancers in 0316-GSC cells. The blue line indicates the linear fit; r indicates Spearman's correlation ($n = 2$ biological replicates for each histone modification and FC value of each gene is the average of the FCs of the two biological replicates).

Figure S4

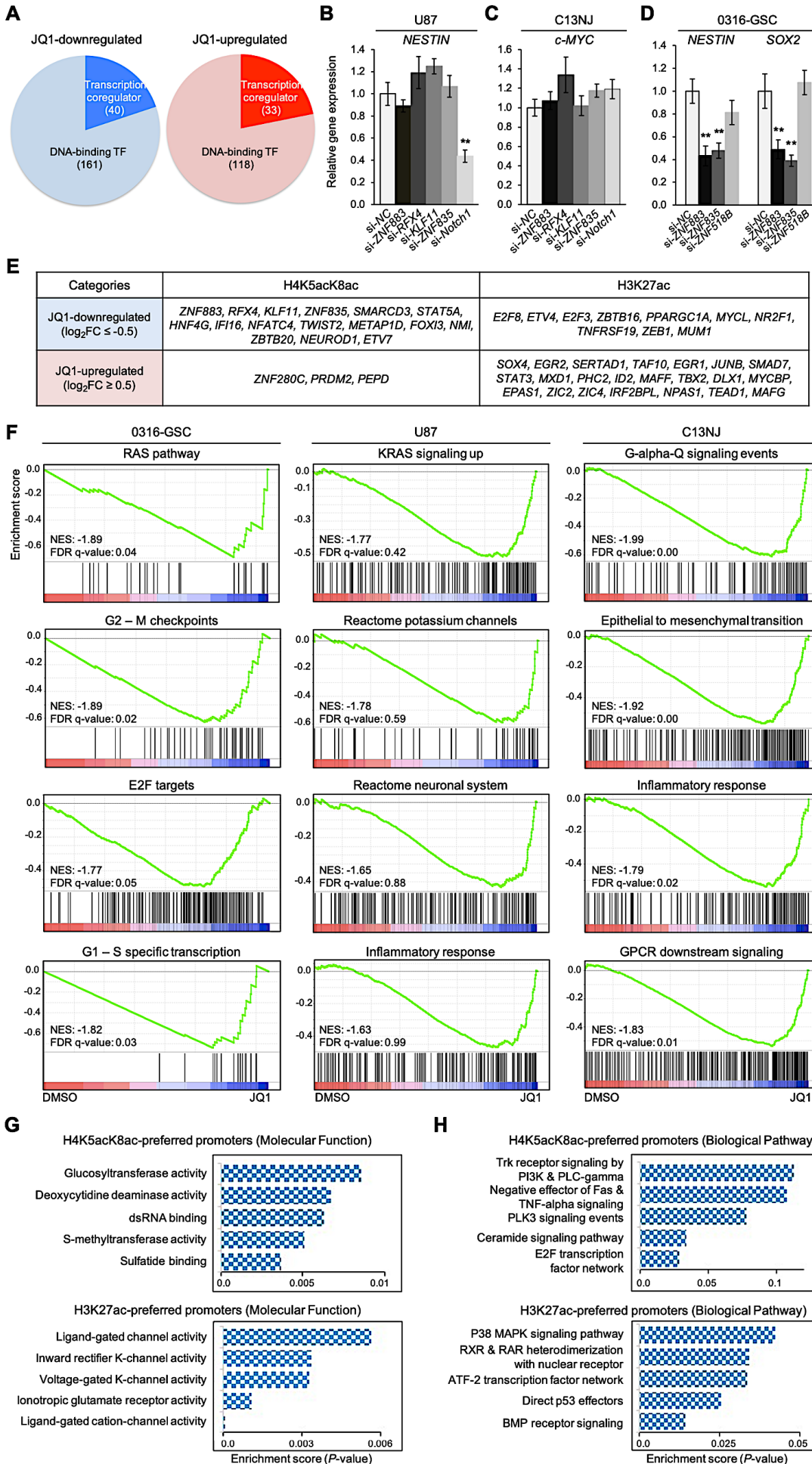


Figure S4. Effect of JQ1 on specific genes and various biological pathways and molecular functions across the three glial cell lines. **A** JQ1-downregulated and upregulated genes involved in transcriptional activity were categorized as transcription coregulators or DNA-binding transcription factors (TFs). **B** and **C** Unlike siRNA knockdown of *NOTCH1*, siRNA knockdown of TF candidate genes with H4K5acK8ac-preferred promoters did not result in significant changes in expression of the stem cell marker gene *NESTIN* in U87 (**B**) cells. Neither siRNA knockdown of *NOTCH1* nor siRNA knockdown of the set of TF candidate genes with H4K5acK8ac-preferred promoters resulted in significant changes in *c-Myc* expression in C13NJ (**C**) cells (n = 3). **D** Comparative siRNA knockdown of selected JQ1-unaffected and JQ1-downregulated genes encoding zinc-finger TFs with H4K5acK8ac-preferred promoters in 0316-GSC. siRNA knockdown of the JQ1-unaffected gene, *ZNF518B*, did not suppress the expression of stem cell marker genes *NESTIN* and *SOX2* (n = 3), but siRNA knockdown of JQ1-downregulated genes, *ZNF833* and *ZNF835*, did significantly suppress the expression of these genes. Data are means \pm SEM. **, $P < 0.01$ (two-tailed Student's *t*-test). **E** JQ1-downregulated and upregulated TF candidate genes are shown categorized according to whether they have H4K5acK8ac- or H3K27ac-preferred promoters in 0316-GSC cells. **F** GSEA results of gene ontology (GO) biological pathways significantly over-represented in the sets of JQ1-downregulated genes in 0316-GSC, U87, and C13NJ are shown (NES; Normalized Enrichment Score). **G** and **H** GO molecular functions (**G**) and biological pathways (**H**) that are significantly over-represented in JQ1-downregulated genes associated with H4K5acK8ac- (upper) or H3K27ac-preferred (lower) promoters in 0316-GSC cells are shown.

Figure S5

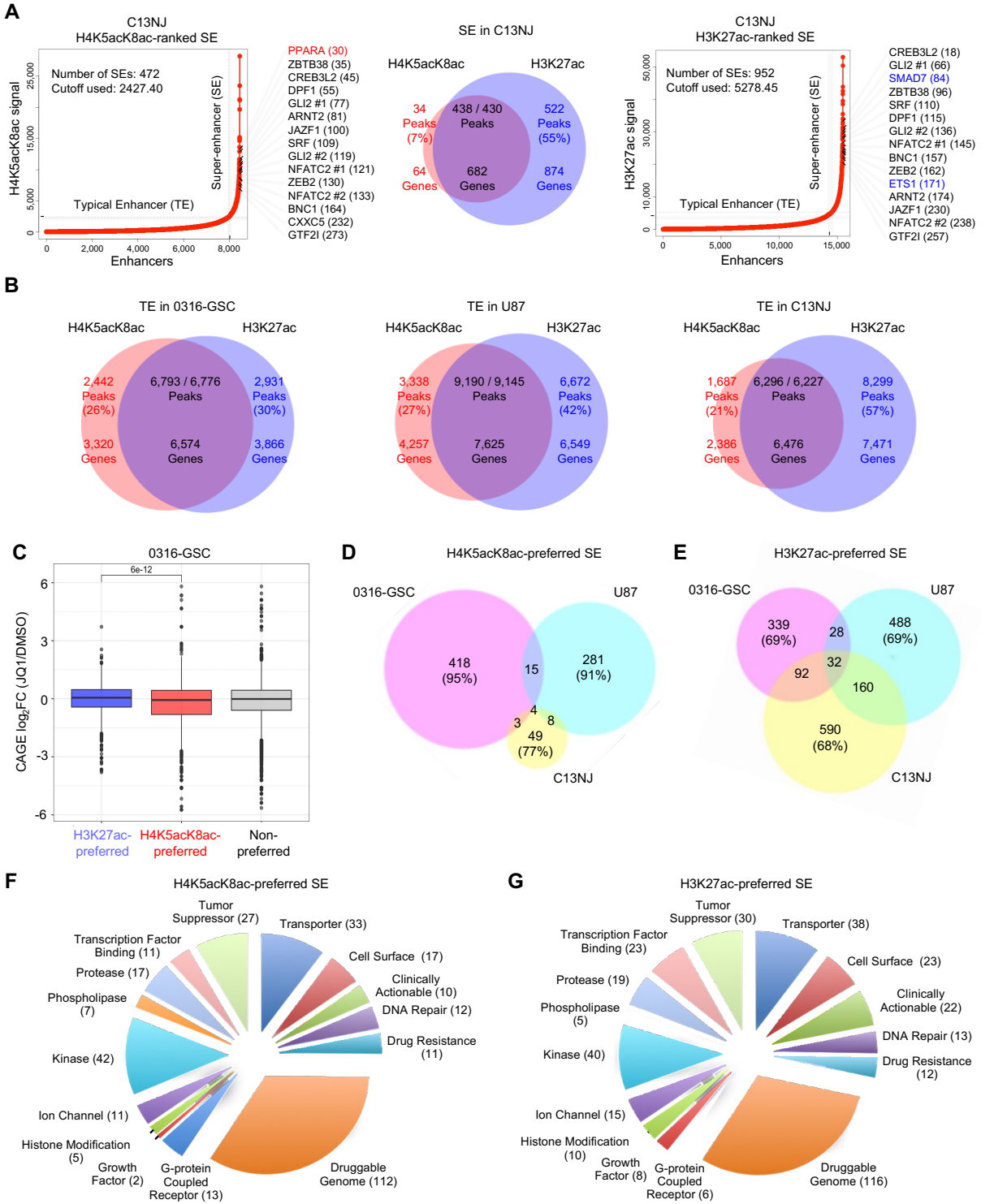


Figure S5 (continued)

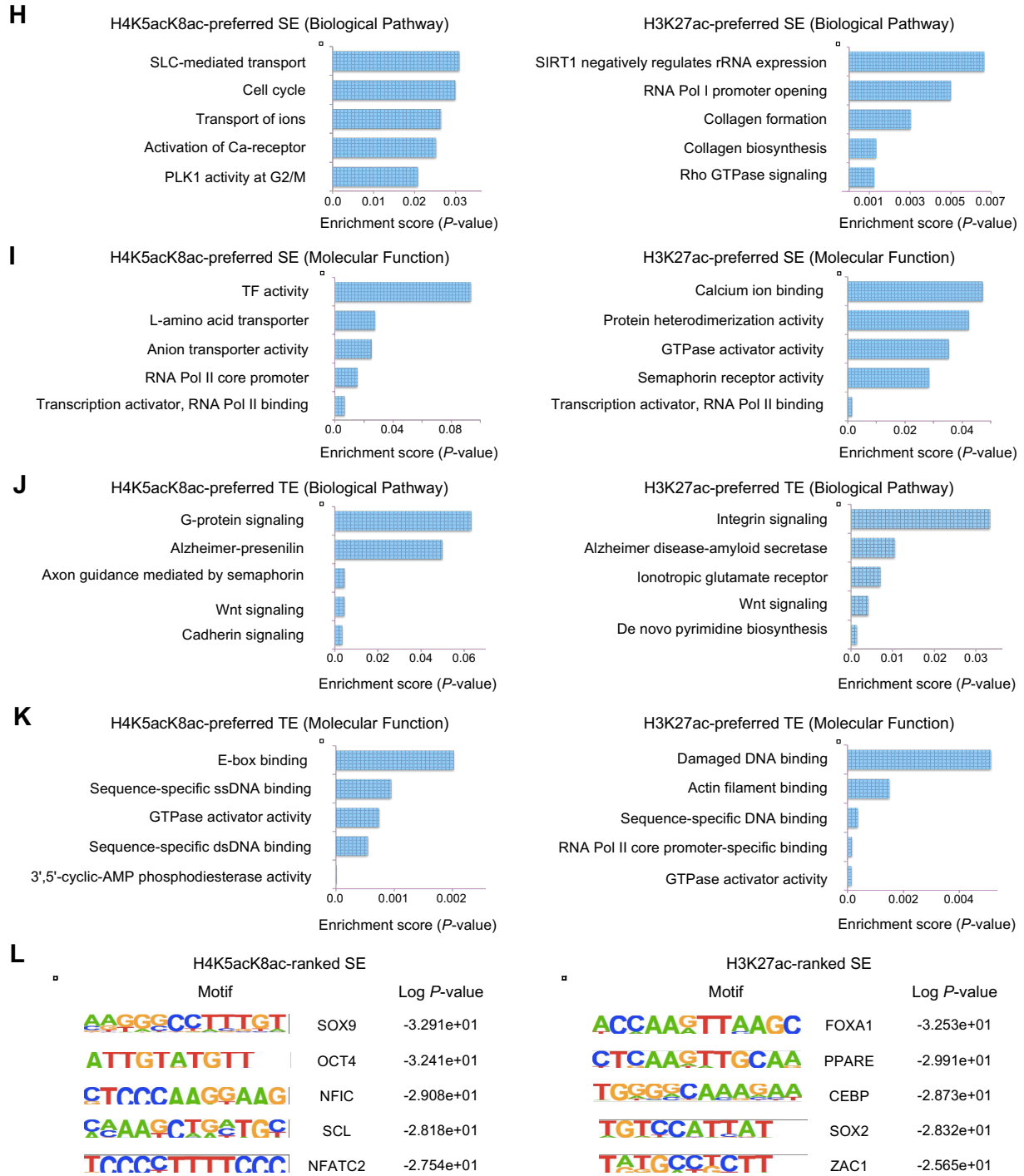


Figure S5. Defining super-enhancers (SEs) by H4K5acK8ac enrichment ranking in 0316-GSC, U87, and C13NJ cells. **A** Enhancers in C13NJ cells were ranked by H4K5acK8ac (left) or H3K27ac (right) signal level by using the ROSE algorithm; those with extremely high signals were defined as SEs (see Methods in the main text for threshold calculations). JQ1-downregulated (*i.e.*, CAGE $\log_2FC < -0.5$) transcription factor (TF) candidate genes with H4K5acK8ac- (red) or H3K27ac-preferred (blue) SEs are shown. Venn diagrams (middle) show the number of peaks and associated genes with H4K5acK8ac- or H3K27ac-preferred SEs or both (the intersection, purple). **B** Venn diagrams of genes with H4K5acK8ac- and/or H3K27ac-preferred typical enhancers (TEs) across three cell lines. **C** Box plots of change in gene expression levels upon JQ1 treatment in 0316-GSC. Genes associated with enhancers (peaks > 1-kb from the TSS) are grouped by the enrichment level of H4K5acK8ac over H3K27ac. The H3K27ac-, H4K5acK8ac-, and non-preferred peaks associated with enhancers are defined by ChIP-seq \log_2FC (H4K5acK8ac/H3K27ac): $\log_2FC < -1$, $\log_2FC > 1$, and $-1 \leq \log_2FC \leq 1$ ($n = 2$ biological replicates for each histone modification and FC value of each gene is the average of the FCs of the two biological replicates). **D** and **E** Venn diagrams showing cell-type specificities of genes with H4K5acK8ac-preferred (**D**) and H3K27ac-preferred (**E**) SEs. **F** and **G** Pie charts of genes with H4K5acK8ac-preferred (**F**) and H3K27ac-preferred (**G**) SEs in 0316-GSC are shown; the genes were identified by integrating the SE-associated genes with information in the Drug-Gene Interaction Database. **H–K** The indicated gene ontology (GO) molecular function and biological pathway categories were over-represented in JQ1-downregulated genes associated with H4K5acK8ac-preferred (left) or H3K27ac-preferred (right) SEs and TEs (**H** and **I**: SEs; **J** and **K**: TEs) in 0316-GSC cells. **L** TF-binding motifs within the H4K5acK8ac (left)- and H3K27ac (right)-ranked SEs. The motifs were found *de novo* by HOMER and then linked to the best matching known motifs. The occurrence panels represent the enrichment of the motif within 500 bp of H4K5acK8ac- and H3K27ac-ranked SEs.

Figure S6

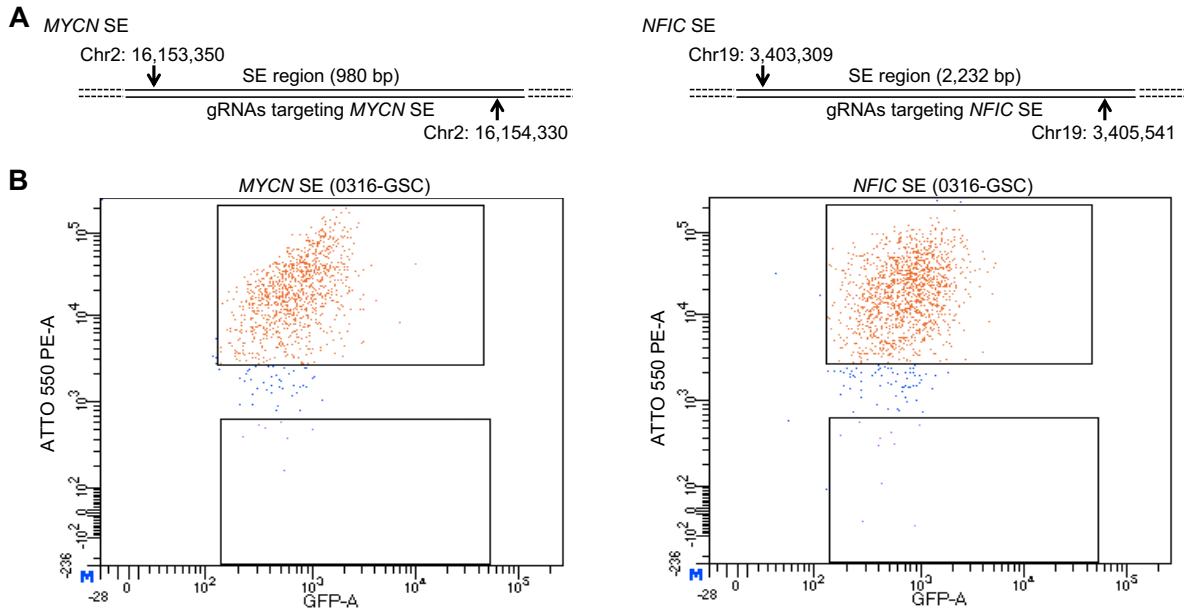


Figure S6. CRISPR-Cas9–mediated genome editing strategy of H4K5acK8ac-preferred super-enhancers (SEs) in 0316-GSC cells. **A** CRISPR-Cas9 knockout strategy for the SEs associated with *MYCN* and *NFIC* in 0316-GSC cells. Guide RNAs (gRNAs; vertical arrows) show the position for deletion of each SE. **B** Fluorescence-activated cell sorting of the SE-edited cells. CRISPR-Cas9–mediated knockout was performed by transfection of a ribonucleoprotein complex consisting of Cas9, crRNA (gRNA), and tracrRNA conjugated with ATTO 550. The sorted ATTO 550 positive cells (upper box) were subjected for further analysis.

Figure S7

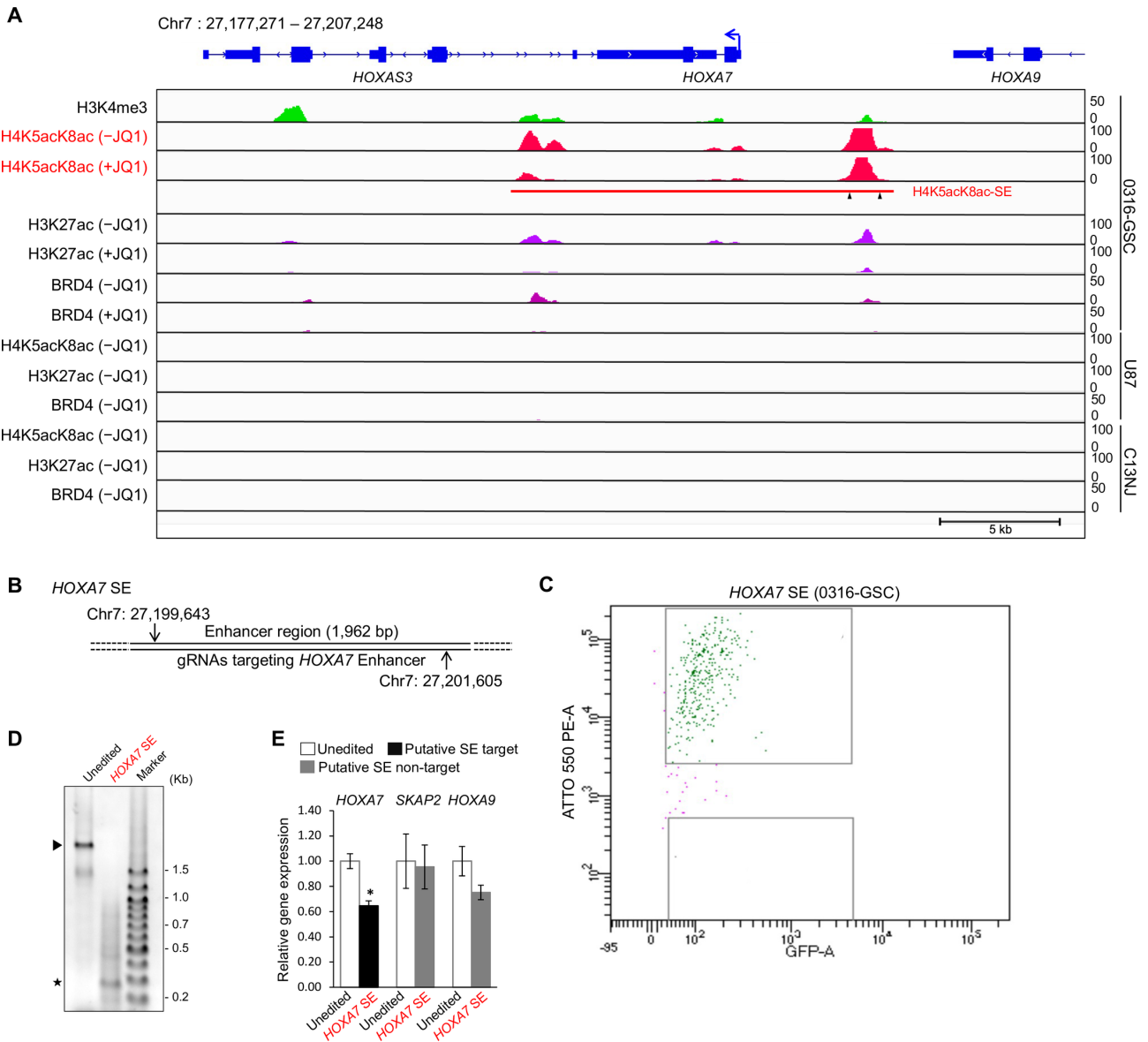


Figure S7. CRISPR-Cas9-mediated genome editing of *HOXA7* SE in 0316-GSC cells. **A** Representative ChIP-seq occupancy tracks of genes with H4K5acK8ac-preferred SE associated with *HOXA7*. The arrowheads under the SE bar show the position for CRISPR-Cas9-mediated deletion of the SE region. ChIP-seq reads were averaged from two biological replicates. **B** CRISPR-Cas9 knockout strategy. Guide RNAs (gRNAs; vertical arrows) show the position for deletion of each enhancer in SE. **C** Fluorescence-activated cell sorting of the SE-edited cells. CRISPR-Cas9-mediated knockout was performed by transfection of a ribonucleoprotein complex consisting of Cas9, crRNA (gRNA), and tracrRNA conjugated with ATTO 550. The sorted ATTO 550 positive cells (upper box) were subjected for further analysis. **D** Expected band sizes of genomic DNA for unedited (arrowhead) and enhancer-edited (asterisk) samples: the results show the deletion of the *HOXA7* SE. Image of the uncropped gel is shown in Figure S9B. **E** RT-qPCR analysis of the expression of putative target TF genes associated with SE and non-target genes (n= 3). Data are means \pm SEM. *, $P < 0.05$ (two-tailed Student's t -test).

Figure S8

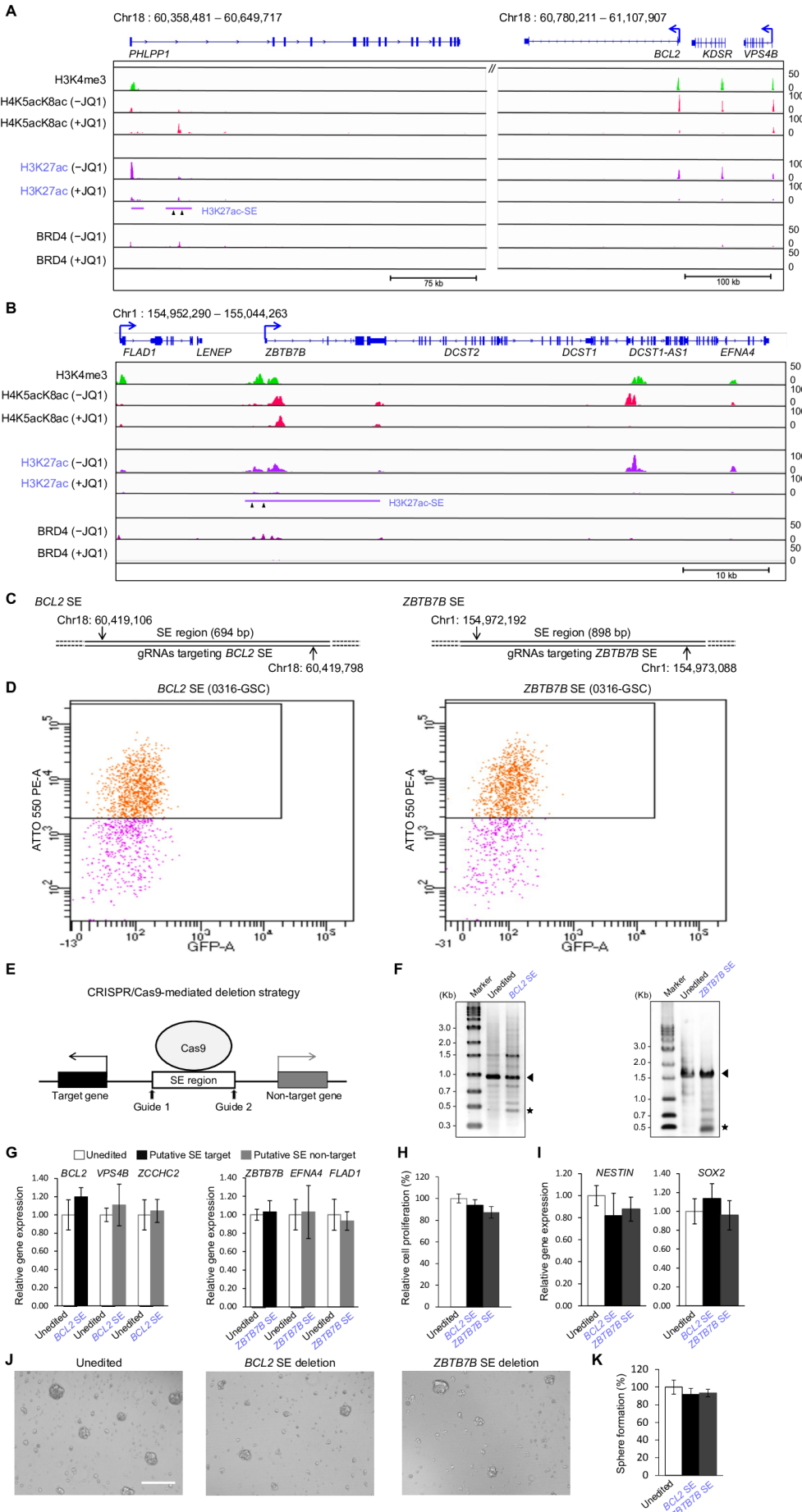


Figure S8. CRISPR-Cas9–mediated genome editing of H3K27ac-preferred super-enhancers (SEs) in 0316-GSC cells. **A** ChIP-seq occupancy tracks of H3K27ac-preferred SEs of *BCL2*. **B** ChIP-seq occupancy tracks of H3K27ac-preferred SEs of *ZBTB7B*. Arrowheads under the SE bar show the position for CRISPR-Cas9–mediated deletion of the SE region. ChIP-seq reads were averaged from two biological replicates. **C** CRISPR-Cas9 knockout strategy. Guide RNAs (gRNAs; vertical arrows) show the position for deletion of each SE. **D** Fluorescence-activated cell sorting of the SE-edited cells. CRISPR-Cas9–mediated knockout was performed by transfection of a ribonucleoprotein complex consisting of Cas9, crRNA (gRNA), and tracrRNA conjugated with ATTO 550. The sorted ATTO 550 positive cells (upper box) were subjected for further analysis. **E** Schematic representation showing the CRISPR-Cas9–mediated genome editing approach for SEs. Guide indicates gRNA. **F** Expected band sizes of genomic DNA for unedited (arrowhead) and SE-edited (asterisk) samples: the results show the deletion of the SE associated with *BCL2* and *ZBTB7B*. Images of the uncropped gel are shown in Figure S9C. **G** RT-qPCR analysis of the expression of putative target TF genes associated with enhancers (En) in SEs and non-target genes (n= 3). **H** Cell proliferation rates at 4 days after SE deletion (n = 4). **I** Expression of stem cell marker genes, *NESTIN* (left) and *SOX2* (right), at 4 days after SE deletion (n = 3). **J** Phase-contrast images of 0316-GSC cells at 14 days after SE deletion. Images are representative of three independent experiments. Scale bar, 50 μ m. **K** *In vitro* sphere formation efficiency of 0316-GSC cells at 2 weeks after SE deletion (n = 3).

Figure S9

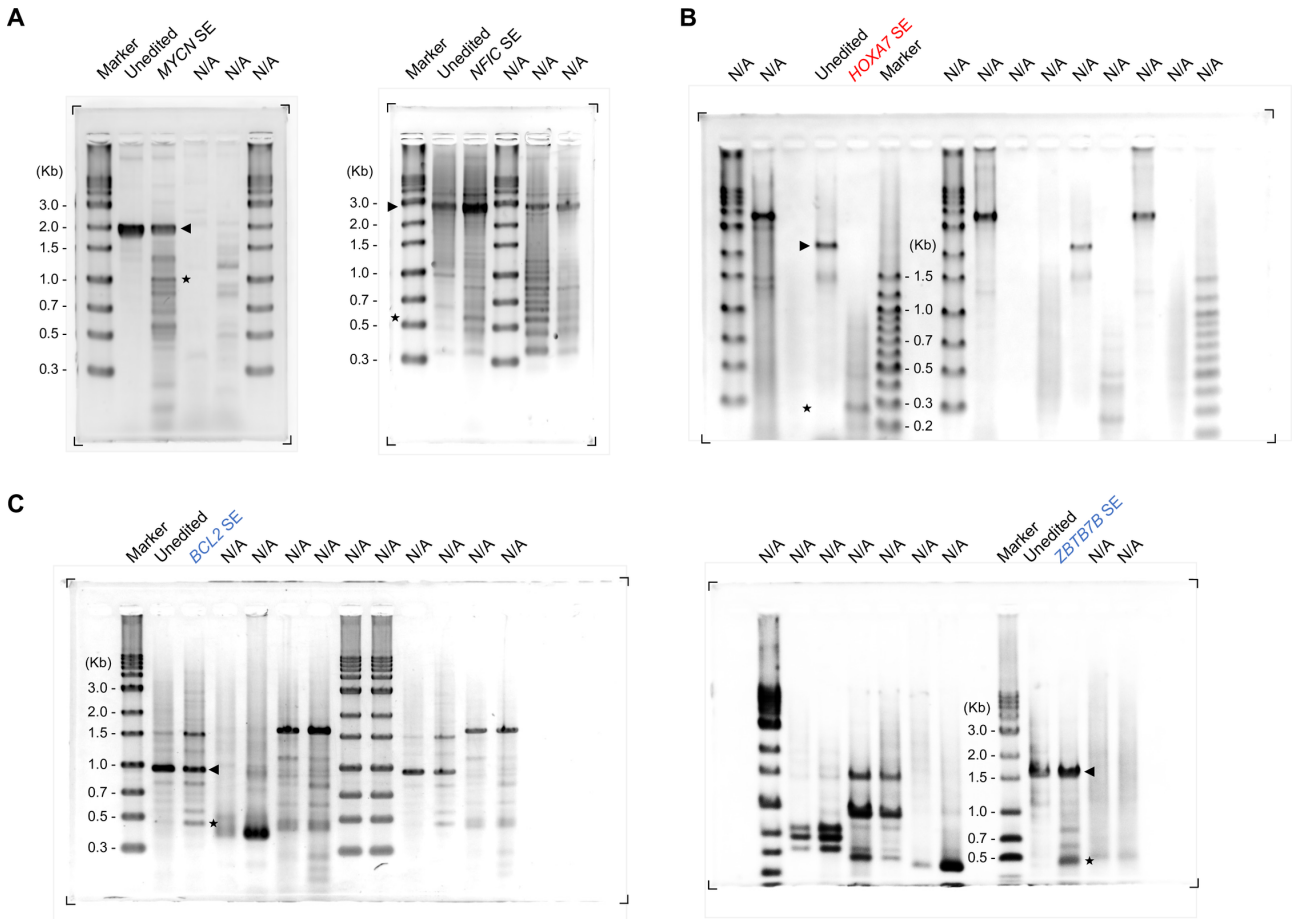


Figure S9. Source data for cropped gel images. A Figure 7B. **B** Figure S7D. **C** Figure S8F. N/A denotes not applicable. Edges of the blots are indicated by black corner brackets.